

# Scaled Quantum Chemical Studies on the Vibrational Spectra of 2-bromo-m-xylene

G.Venkatesh<sup>1</sup>, M.Govindaraju<sup>2\*</sup> and P.Vennila<sup>3</sup>

<sup>1</sup>Research and Development Centre, Bharathiar University, Coimbatore - 641 046, India.

<sup>2</sup>Department of Chemistry, Kongu Polytechnic College, Erode- 638052, India.

<sup>3</sup>Department of Chemistry, Thiruvalluvar Govt. Arts College, Rasipuram, Tamilnadu, India.

## ARTICLE INFO

### Article history:

Received: 12 December 2013;

Received in revised form:

14 February 2014;

Accepted: 19 February 2014;

### Keywords

Normal Coordinate Analysis, FT-IR, Density Functional Theory, HOMO, LUMO, First-order Hyperpolarizability, Mulliken population analysis, Electronic Excitation Energy.

## ABSTRACT

The FT-IR and FT-Raman spectra of 2-bromo-m-xylene (2BMX) have been recorded in the regions 4000–400  $\text{cm}^{-1}$  and 4000–100  $\text{cm}^{-1}$ , respectively. The fundamental vibrational frequencies and intensities of the vibrational bands were evaluated using density functional theory (DFT) using standard B3LYP method and 6-311+G\*\* basis set combinations. The vibrational spectra were interpreted, with the aid of normal coordinate analysis based on a scaled quantum mechanical force field. The Infrared and Raman spectra were also predicted from the calculated intensities. The Mulliken population analysis of the molecule is computed by using DFT calculations. The calculated HOMO and LUMO energies shows that charge transfer occur within the molecule. Further, density functional theory (DFT) combined with quantum chemical calculations to determine the first-order hyperpolarizability. Electronic excitation energies, oscillator strength and nature of the respective excited states were calculated by the closed-shell singlet calculation method were also calculated for the molecule.

© 2014 Elixir All rights reserved.

## Introduction

Xylene areas of applications include printing, rubber, and leather industries. It is a common component of ink, rubber, adhesive, and leather industries.

In thinning paints and varnishes, it can be substituted for toluene where slower drying is desired, and thus is used by conservators of art objects in solubility testing. 2-Bromo-m-xylene, is an organic building block used for the synthesis of various chemicals. It can be used for the preparation of Pd(II) complexes used as catalyst.

Quantum chemical computational methods have proved to be an essential tool for interpreting and predicting the vibrational spectra. A significant advance in this area was made by scaled quantum mechanical (SQM) force field method [1-3]. In scaled quantum mechanical (SQM) approach, the systematic errors of the computed harmonic force field are corrected by a few scale factors which are found to be well transferable between chemically related molecules and were recommended for general use. Recent spectroscopic studies on these materials have been motivated because the vibrational spectra are very useful for the understanding of specific biological process and in the analysis of relatively complex systems.

In this work, we apply the density functional theory to study the vibrational spectra and structure of 2-bromo-m-xylene (2BMX). The calculated Infrared and Raman spectra of the title compounds were also stimulated utilizing the scaled force fields and the computed dipole derivatives for IR intensities and polarisability derivatives for Raman intensities.

## Experimental Details

The sample of 2BMX was purchased from the Sigma-Aldrich Chemical Company (USA) with a stated purity of greater than 98% and it was used as such without further purification. The FT-Raman spectrum of 2BMX has been recorded using 1064 nm line of Nd:YAG laser as excitation

wavelength in the region 4000-100  $\text{cm}^{-1}$  on a Bruker model IFS 66V spectrophotometer equipped with FRA 106 FT-Raman module accessory. The FT-IR spectrum of this compound was recorded in the region 4000–400  $\text{cm}^{-1}$  on IFS 66V spectrophotometer.

## Computational Details

All calculations were performed using GAUSSIAN 09W program package [4] and the vibrational modes were assigned by means of visual inspection using GAUSSVIEW program and also from the results of normal co-ordinate calculations. The geometry optimization and energy calculations of conformers of 2BMX were carried out using DFT (B3LYP) methods [5,6] with 6-31G\* and 6-311+G\*\* basis sets, respectively. The Cartesian representation of the theoretical force constants have been computed at optimized geometry by assuming  $C_s$  point group symmetry, scaling of the force fields were performed by the scaled quantum mechanical procedure [7].

The symmetry of the molecule was also helpful in making vibrational assignments. The symmetries of the vibrational modes were determined by using the standard procedure [8] of decomposing the traces of the symmetry operation into the irreducible representations. The symmetry analysis for the vibrational mode of 2BMX is presented in some details in order to describe the basis for the assignments. By combining the results of the GAUSSVIEW program with symmetry considerations, vibrational frequency assignments were made with a high degree of confidence.

The prediction of Raman intensities was carried out by following the procedure outlined below. The Raman activities ( $S_i$ ) calculated by the GAUSSIAN 09W program and adjusted during scaling procedure with MOLVIB were converted to relative Raman intensities ( $I_i$ ) using the following relationship derived from the basic theory of Raman scattering [9–10].

$$I_i = \frac{f(v_o - v_i)^4 S_i}{v_i [1 - \exp(-hcv_i / KT)]} \text{-----(1)}$$

Where  $v_o$  is the exciting frequency (in  $\text{cm}^{-1}$ ),  $v_i$  is the vibrational wavenumber of the  $i^{\text{th}}$  normal mode;  $h$ ,  $c$  and  $k$  are fundamental constants, and  $f$  is a suitably chosen common normalization factor for all peak intensities.

#### Essentials of nonlinear optics related to $\beta$

The nonlinear response of an isolated molecule in an electric field  $E_i(\omega)$  can be represented as a Taylor expansion of the total dipole moment  $\mu_i$  induced by the field:

$$\mu_i = \mu_0 + \alpha_{ij} E_j + \beta_{ijk} E_i E_j + \dots$$

Where  $\alpha$  is linear polarizability,  $\mu_0$  the permanent dipole moment and  $\beta_{ijk}$  are the first-order hyperpolarizability tensor components. The components of first-order hyperpolarizability can be determined using the relation

$$\beta_i = \beta_{iii} + \frac{1}{3} \sum_{i \neq j} (\beta_{ijj} + \beta_{jij} + \beta_{jji})$$

Using the x, y and z components the magnitude of the total static dipole moment ( $\mu$ ), isotropic polarizability ( $\alpha_0$ ), first-order hyperpolarizability ( $\beta_{\text{total}}$ ) tensor, can be calculated by the following equations:

$$\mu_1^0 = (\mu_x^2 + \mu_y^2 + \mu_z^2)^{1/2}$$

$$\beta_{\text{tot}} = (\beta_x^2 + \beta_y^2 + \beta_z^2)^{1/2}$$

The complete equation for calculating the first-order hyperpolarizability from GAUSSIAN 09W output is given as follows:

$$\beta_{\text{tot}} = [(\beta_{xxx} + \beta_{yyy} + \beta_{zzz})^2 + (\beta_{yyy} + \beta_{zzz} + \beta_{yxx})^2 + (\beta_{zzz} + \beta_{xxx} + \beta_{zyy})^2]$$

The  $\beta$  components of GAUSSIAN 09W output are reported in atomic units, the calculated values have to be converted into electrostatic units ( $1 \text{ a.u.} = 8.3693 \times 10^{-33} \text{ esu}$ ).

Molecular geometries were fully optimized by Berny's optimization algorithm using redundant internal coordinates. All optimized structures were confirmed to be minimum energy conformations. An optimization is complete when it has converged, i.e., when it has reached a minimum on the potential energy surface, thereby predicting the equilibrium structures of the molecules. This criterion is very important in geometry optimization. The inclusion of d polarization and double zeta function in the split valence basis set is expected to produce a marked improvement in the calculated geometry. At the optimized structure, no imaginary frequency modes were obtained proving that a true minimum on the potential energy surface was found. The electric dipole moment and dispersion free first-order hyperpolarizability were calculated using finite field method. The finite field method offers a straight forward approach to the calculation of hyperpolarizabilities. All the calculations were carried out at the DFT level using the three-parameter hybrid density functional B3LYP and a 6-311+G\*\* basis set.

## Results and discussion

### Structural description

The optimized molecular structure with the numbering of atoms of the title compound is shown in Fig 1. In order to find the most optimized geometry, the energy calculations were carried out for 2BMX, using B3LYP/6-31G\* and B3LYP/6-311+G\*\* methods. The total energies obtained for were listed in Table 1. It is clear from the Table 1 the structure optimizations have shown that the B3LYP/6-311+G\*\* have produced the

global minimum energy. The most optimized structural parameters were also calculated and they were depicted in Table 2.

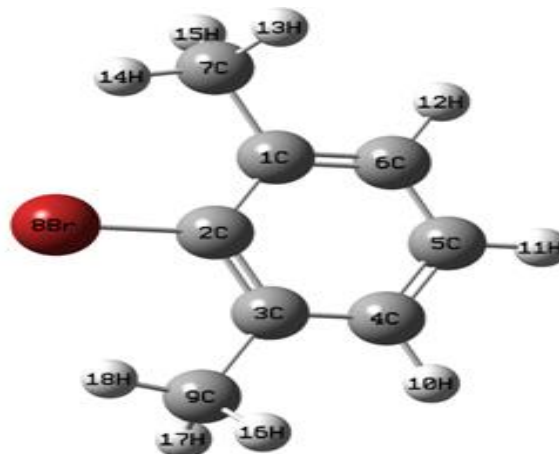


**Fig 1. The optimized molecular structure of 2BMX**  
**Table 1. Total energies of 2BMX, calculated at DFT B3LYP/6-31G\* and B3LYP/6-311+G\*\* level**

Method	Energies (Hartrees)
6-31G*	-2881.84512378
6-311+G**	-2881.99203957

Normal coordinate analysis were carried out to provide a complete assignment of the fundamental vibrational frequencies for the molecule for this purpose the full set of standard internal coordinates (containing-redundancies) were defined as given Table 3. From these a non-redundant set local symmetry coordinates were constructed by suitable linear combinations of internal coordinates following the recommendations of Fogarasi and Pulay [11] and they are presented in Table 4. The theoretically calculated force field were transformed to this later set of vibrational coordinates and used in all subsequent calculations.

### Vibrational assignment

The molecule under consideration would belong to  $C_s$  point group and the 48 normal mode of fundamental vibrations, which span the irreducible representation  $33A' + 15A''$ . The  $A'$  modes be polarized while the  $A''$  modes be depolarized in the Raman spectrum. The harmonic vibrational modes calculated for 2BMX along with reduced mass, force constants Infrared intensities and Raman scattering activities have been summarized in Table 5. The FT-IR and FT-Raman spectra of 2BMX are shown in Fig 2 and Fig 3, respectively.

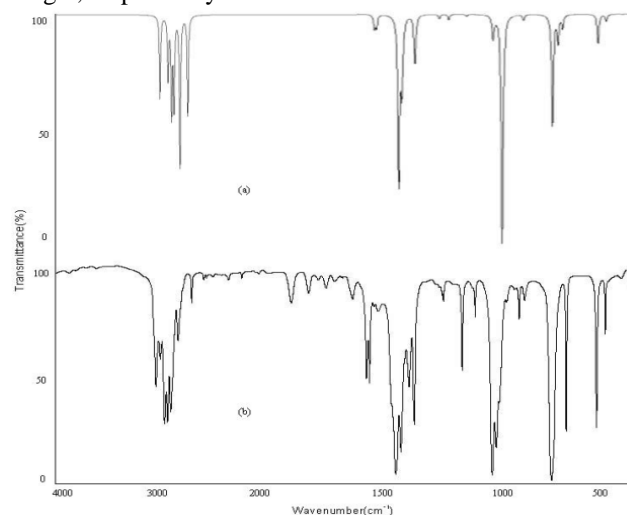


**Fig 2. FT-IR spectra of 2BMX**  
**(a) Calculated (b) Observed with B3LYP/6-311+G\*\***

Table 2. Optimized geometrical parameters of 2BMX obtained by B3LYP/6-311+G\*\* density functional calculations

Bond length	Value(Å)	Bond angle	Value(Å)	Dihedral angle	Value(Å)
C2-C1	1.38599	C3-C2-C1	119.99953	C4-C3-C2-C1	0.00000
C3-C2	1.38599	C4-C3-C2	120.00023	C5-C4-C3-C2	0.00000
C4-C3	1.38600	C5-C4-C3	120.00023	C6-C5-C4-C3	0.00000
C5-C4	1.38599	C6-C5-C4	119.99953	C7-C1-C2-C3	-179.42433
C6-C5	1.38599	C7-C1-C2	119.99704	Br8-C2-C1-C6	179.42498
C7-C1	1.53999	Br8-C2-C1	119.99898	C9-C3-C2-C1	-179.42864
Br8-C2	1.90997	C9-C3-C2	119.99892	H10-C4-C3-C2	179.42806
C9-C3	1.54007	H10-C4-C3	119.99826	H11-C5-C4-C3	179.42800
H10-C4	1.12205	H11-C5-C4	119.99899	H12-C6-C5-C4	179.42803
H11-C5	1.12194	H12-C6-C5	119.99647	H13-C7-C1-C2	119.99857
H12-C6	1.12197	H13-C7-C1	109.50263	H14-C7-C1-C2	-0.07432
H13-C7	1.12199	H14-C7-C1	109.50197	H15-C7-C1-C2	-119.93039
H14-C7	1.12201	H15-C7-C1	109.49631	H16-C9-C3-C2	-119.99963
H15-C7	1.12205	H16-C9-C3	109.49851	H17-C9-C3-C2	119.92986
H16-C9	1.12198	H17-C9-C3	109.49622	H18-C9-C3-C2	0.07004
H17-C9	1.12203	H18-C9-C3	109.50003		
H18-C9	1.12193				

\*for numbering of atom refer Fig 1

Table 3. Definition of internal coordinates of 2BMX

No(i)	symbol	Type	Definition
Stretching 1-6	r <sub>i</sub>	C-C	C1-C2,C2-C3,C3-C4,C4-C5,C5-C6,C6-C1
7-9	S <sub>i</sub>	C-H	C4-H10,C5-H11,C6-H12
10	p <sub>i</sub>	C-Br	C2-Br8
11-12	P <sub>i</sub>	C-C(m)	C3-C9,C1-C7
13-15	n <sub>i</sub>	C-H(m)	C7-H13,C7-H14,C7-H15
16-18	N <sub>i</sub>	C-H(m)	C9-H16,C9-H17,C9-H18
Bending 19-24	α <sub>i</sub>	C-C-C	C1-C2-C3,C2-C3-C4,C3-C4-C5, C4-C5-C6,C5-C6-C1,C6-C1-C2
25-30	θ <sub>i</sub>	C-C-H	C3-C4-H10,C5-C4-H10,C4-C5-H11,C6-C5-H11,C5-C6-H12, C1-C6-H12
31-32	β <sub>i</sub>	C-C-Br	C1-C2-Br8,C3-C2-Br8
33-36	Φ <sub>i</sub>	C-C-C	C6-C1-C7,C2-C1-C7,C2-C3-C9, C4-C3-C9
37-39	μ <sub>i</sub>	H-C-H	H13-C7-H14,H14-C7-H15, H15-C7-H13
40-42	v <sub>i</sub>	C-C-H	C1-C7-H13,C1-C7-H14,C1-C7-H15
43-45	ε <sub>i</sub>	H-C-H	H16-C9-H17,H17-C9-H18, H18-C9-H16
46-48	ι <sub>i</sub>	C-C-H	C3-C9-H16,C3-C9-H17,C3-C9-H18
Out-of-plane 49-51	ω <sub>i</sub>	C-H	H10-C4-C3-C5,H11-C5-C4-C6, H12-C6-C5-C1.
52	ξ <sub>i</sub>	C-Br	Br8-C2-C3-C1
53-54	Ω <sub>i</sub>	C-C	C9-C3-C4-C2,C7-C1-C2-C6
Torsion 55-60	τ <sub>i</sub>	C-C	C1-C2-C3-C4,C2-C3-C4-C5,C3-C4-C5-C6,C4-C5-C6-C1,C5-C6-C1-C2,C6-C1-C2,C3
61	τ <sub>i</sub>	C-H	C2-C1-C7-(H13,H14,H15)
62	τ <sub>i</sub>	C-H	C4-C3-C9-(H16,H17,H18)

\*for numbering of atom refer Fig 1

Table 4. Definition of local symmetry coordinates and the value corresponding scale factors used to correct the force fields for 2BMX

No.(i)	Symbol <sup>a</sup>	Definition <sup>b</sup>	Scale factors used in calculation
1-6	C-C	r1,r2,r3,r4,r5,r6	0.914
7-9	C-H	S7,S8,S9	0.914
10	C-Br	p10	0.992
11-12	C-C(m)	P11,P12	0.992
13	mss1	(n13+n14+n15)/√3	0.995
14	mips1	(2n14-n13-n15)/√6	0.992
15	mops1	(n14-n15)/√2	0.919
16	mss2	(N16+N17+N18)/√3	0.919
17	mips2	(2N17-N16-N18)/√6	0.919
18	mops2	(N17-N18)/√2	0.919
19	C-C-C	(α19-α20+α21-α22+α23-α24)/√6	0.992
20	C-C-C	(2α19-α20-α21+2α22-α23-α24)/√12	0.992
21	C-C-C	(α20-α21+α23-α24)/2	0.992
22-24	C-C-H	(θ25-θ26)/√2,(θ27-θ28)/√2,(θ29-θ30)/√2	0.916
25	C-C-Br	(β31-β32)/√2,	0.923
26-27	C-C-C	(Φ33-Φ34)/√2,(Φ35-Φ36)/√2	0.923

28	msb1	$(\mu37+\mu38+\mu39-v40-v41-v42)/\sqrt{6}$	0.990
29	mipb1	$(2\mu39-\mu37-\mu38)/\sqrt{6}$	0.990
30	mopb1	$(\mu37-\mu39)/\sqrt{2}$	0.990
31	mipr1	$(2v41-v40-v42)/\sqrt{6}$	0.990
32	mopr1	$(v40-v42)/\sqrt{2}$	0.990
33	msb2	$(\varepsilon43+\varepsilon44+\varepsilon45-i46-i47-i48)/\sqrt{6}$	0.990
34	mipb2	$(2\varepsilon45-\varepsilon43-\varepsilon44)/\sqrt{6}$	0.990
35	mopb2	$(\varepsilon43-\varepsilon45)/\sqrt{2}$	0.990
36	mipr2	$(2i47-i46-i48)/\sqrt{6}$	0.990
37	mopr2	$(i46-i48)/\sqrt{2}$	0.990
38-40	C-H	$\omega49, \omega50, \omega51$	0.994
41	C-Br	$\xi52$	0.962
42-43	C-C	$\Omega53, \Omega54$	0.962
44	tring	$(\tau55-\tau56+\tau57-\tau58+\tau59-\tau60)/\sqrt{6}$	0.994
45	tring	$(\tau55-\tau57+\tau58-\tau60)/2$	0.994
46	tring	$(-\tau55+2\tau56-\tau57-\tau58+2\tau59-\tau60)/\sqrt{12}$	0.994
47	m1	$\tau61/3$	0.979
48	m2	$\tau62/3$	0.979

<sup>a</sup> These symbols are used for description of the normal modes by TED in Table 5.

<sup>b</sup> The internal coordinates used here are defined in Table 3.

**Table 5. Detailed assignments of fundamental vibrations of 2BMX by normal mode analysis based on SQM force field calculation**

S. No.	Symmetry species C <sub>s</sub>	Observed frequency (cm <sup>-1</sup> )		Calculated frequency (cm <sup>-1</sup> ) with B3LYP/6-311+G <sup>**</sup> force field				TED (%) among type of internal coordinates <sup>c</sup>
		Infrared	Raman	Unscaled	Scaled	IR <sup>a</sup> A <sub>i</sub>	Raman <sup>b</sup> I <sub>i</sub>	
1	A'	3254	3253	3251	3249	20.510	67.574	CH(99)
2	A'			3195	3192	15.470	66.375	CH(99)
3	A'	3171		3169	3167	23.969	233.773	CH(99)
4	A'		3154	3155	3150	22.127	74.106	mips2(47),mops1(38),mips1(12)
5	A'			3143	3141	0.022	68.831	mips2(51),mops1(35),mips1(12)
6	A'	3112	3111	3110	3108	11.237	196.479	mips1(49),mops2(34),mops1(16)
7	A'			3111	3107	26.438	66.737	mops2(65),mips1(26),mops1(9)
8	A'	3057		3056	3053	13.564	65.584	mss2(49),mss1(49)
9	A'			3054	3052	11.455	62.331	mss1(49),mss2(49)
10	A'		1649	1648	1645	3.297	15.367	CC(70),bCH(12),bring(10)
11	A'			1640	1636	3.049	18.791	CC(60),bCH(19),bring(8)
12	A'	1536		1534	1529	19.646	10.877	bmopb2(52),bmipb2(40)
13	A'		1531	1530	1528	22.588	5.965	bmipb1(54),bmopb2(11),bmipb2(8),CC(8),bCH(7)
14	A'	1517		1519	1516	10.149	16.003	bmopb2(40),bmipb2(23),bCH(12),CC(10),bmopr2(8)
15	A'		1514	1517	1513	8.201	17.960	bmopb1(58),bmipb1(41)
16	A'			1506	1504	1.070	1.349	bmipb2(45),bCH(18),bmopb2(17),CC(11)
17	A'	1458		1456	1453	6.772	7.970	bmipb2(28),CC(20),bmopb2(19),bCH(8),bmsb1(6),bmipb1(5)
18	A'		1454	1453	1450	5.341	16.623	bmsb2(41),bmsb1(28),CCm(11),CC(10)
19	A'			1452	1448	0.924	17.866	bmsb1(47),bmsb2(37),CCm(7)
20	A''	1339		1337	1334	1.142	5.666	gCC(84),bCH(6)
21	A'		1293	1292	1290	0.214	18.726	CCm(40),CC(24),bCH(15),bring(14)
22	A'			1293	1289	1.173	2.120	bCH(44),CC(19),CCm(13)
23	A'	1210		1206	1204	0.509	6.213	bCH(73),CC(21),CCm(5)
24	A''		1145	1144	1141	0.087	5.318	gCC(44),bCH(35)
25	A''			1084	1079	0.837	0.625	gCC(39),bmopb1(14),bmipb1(12),bmopr1(9),bmopr2(8),bmipr1(8)
26	A''	1078		1079	1077	4.998	0.774	tring(52),bmopr2(11),gCC(10),bmipr1(8),gCH(5)
27	A'		1070	1069	1066	0.642	0.387	bmipr2(29),bmopr1(19),CCm(14),CC(13),bmipb2(9),bmopb2(7)
28	A'			1037	1034	57.084	7.846	bring(51),CC(24),CBr(18)
29	A'	1026		1025	1023	3.608	6.149	bmopr1(27),bmipr2(25),CC(19),bmipb2(8),bmipr1(7),bmopb2(6)
30	A''		983	982	980	0.127	0.081	gCH(86),tring(12)
31	A'			935	931	1.439	0.379	CCm(40),CC(21),bring(13),bmipr2(6),bmopr1(5)
32	A''	910		908	905	0.000	2.729	gCH(88)
33	A''		798	796	792	27.634	2.135	gCH(80),tring(10)
34	A'	769		768	766	6.637	5.462	bring(57),CCm(18),CC(12),CBr(10)
35	A''			746	744	3.269	1.281	tring(61),gCC(17),gCBr(14),gCH(6)
36	A'		577	578	574	7.224	18.244	bring(35),CCm(23),CC(21),CBr(19)
37	A''	542		540	537	0.000	0.014	gCC(53),tring(40)
38	A'			539	535	1.715	5.449	bring(77),CCm(10),bCBr(6)
39	A''	526	525	524	522	0.036	0.354	tring(59),gCBr(23),gCH(11),gCC(5)

40	A'			462	458	0.051	0.259	bCC2(41),bCC1(29),bCBr(16),CC(5)
41	A'		366	364	360	0.230	4.304	bCC1(32),CBr(31),bCC2(18),bring(7)
42	A'			259	257	2.052	1.974	CBr(32),bCC1(22),bring(20),bCC2(18),CC(5)
43	A''		256	254	251	4.386	2.710	gCC(44),gCBr(42),gCH(6)
44	A''			236	234	0.001	3.508	tring(66),gCH(14),gCC(10)
45	A'		218	216	213	0.163	0.502	bCBr(85),bCC1(7)
46	A''			162	159	0.409	0.214	tm2(65),tm1(25)
47	A''		161	158	154	0.018	0.098	tm1(55),tm2(26),gCC(5)
48	A''			109	106	0.374	1.495	tring(84)

Abbreviations used: b, bending; g, wagging; t, torsion; s, strong; vs, very strong; w, weak; vw, very weak;

<sup>a</sup> Relative absorption intensities normalized with highest peak absorption

<sup>b</sup> Relative Raman intensities calculated by Eq 1 and normalized to 100.

<sup>c</sup> For the notations used see Table 4.

**Table 6. Mullikan's atomic charges of 2BMX based on B3LYP/6-311+G\*\* method**

S.No	Atom No.	B3LYP/6-311+G**
1	C1	-0.012474
2	C2	0.271588
3	C3	-0.012421
4	C4	-0.059316
5	C5	0.011353
6	C6	-0.059293
7	C7	0.067374
8	Br8	-0.259915
9	C9	0.067358
10	H10	0.009642
11	H11	0.013762
12	H12	0.009650
13	H13	-0.009241
14	H14	-0.012552
15	H15	-0.001864
16	H16	-0.012498
17	H17	-0.009253
18	H18	-0.001899

**Table 7. The dipole moment ( $\mu$ ) and first-order hyperpolarizability ( $\beta$ ) of 2BMX derived from DFT calculations**

$\beta_{xxx}$	66.316
$\beta_{xyy}$	-12.165
$\beta_{xyx}$	315.74
$\beta_{yyx}$	-2046.9
$\beta_{yxx}$	15.173
$\beta_{xzz}$	-2659.1
$\beta_{zyz}$	-182.36
$\beta_{xzz}$	22.098
$\beta_{vzz}$	4883.4
$\beta_{zzz}$	-66.214
$\beta_{total}$	1.0574
$\mu_x$	0.29900074
$\mu_y$	1.7154E-05
$\mu_z$	0.09966213
$\mu$	0.63141114

Dipole moment ( $\mu$ ) in Debye, hyperpolarizability  $\beta(-2\omega;\omega,\omega)$   $10^{-30}$ esu.

**Table 8. Computed absorption wavelength ( $\lambda_{ng}$ ), energy ( $E_{ng}$ ), oscillator strength ( $f_n$ ) and its major contribution**

n	$\lambda_{ng}$	$E_{ng}$	$f_n$	Major contribution
1	199.8	6.21	0.0008	H-1->L+1(+51%), H-0->L+0(+45%)
2	195.4	6.35	0.0004	H-1->L+0(+52%), H-0->L+1(42%)
3	186.4	6.65	0.0010	H-0->L+2(+86%)

(Assignment; H=HOMO,L=LUMO,L+1=LUMO+1,etc.)

Root mean square (RMS) values of frequencies were obtained in the study using the following expression,

$$RMS = \sqrt{\frac{1}{n-1} \sum_i^n (u_i^{calc} - u_i^{exp})^2}$$

The RMS error of the observed and calculated frequencies (unscaled / B3LYP/6-311+G\*\*) of 2BMX was found to be 97  $cm^{-1}$ . This is quite obvious; since the frequencies calculated on the basis of quantum mechanical force fields usually differ appreciably from observed frequencies. This is partly due to the neglect of a harmonicity and partly due to the approximate nature of the quantum mechanical methods.

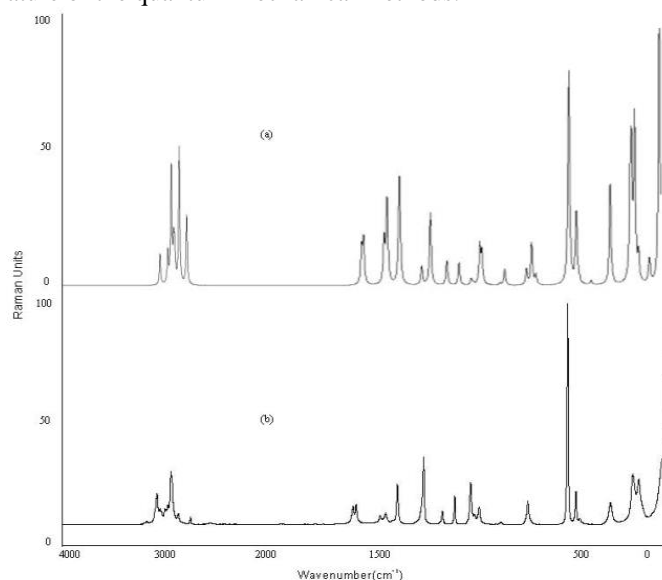
subsequent least square fit refinement algorithm resulted into a very close agreement between the observed fundamentals and the scaled frequencies. Refinement of the scaling factors applied in this study achieved a weighted mean deviation of 7.48  $cm^{-1}$  between the experimental and scaled frequencies of the title compound.

#### C-H vibrations

Aromatic compounds commonly exhibit multiple weak bands in the region 3300–3100  $cm^{-1}$  due to aromatic C–H stretching vibrations. Accordingly, in the present study the C–H vibrations of the title compounds are observed at 3254, 3171, 3169 and 3167  $cm^{-1}$  in the FTIR spectrum and 3253, 3251 and 3249  $cm^{-1}$  in Raman for 2BMX. The bands due to C–H in-plane ring bending vibration interacting with C–C stretching vibration are observed as a number of m-w intensity sharp bands in the region 1300–1000  $cm^{-1}$ . C–H out-of-plane bending vibrations are strongly coupled vibrations and occur in the region 900–667  $cm^{-1}$ . The in-plane and out-of-plane bending vibrations of C–H have also been identified for the title compound.

#### Ring vibrations

The aromatic ring modes predominantly involve C–C bonds. The vibrational frequency 1756-1608  $cm^{-1}$  corresponds to stretching and contraction of the other part of the ring. Here the scaled value of 1645  $cm^{-1}$  is in excellent agreement with the reported value [12]. The scaled frequencies of 366, 364 and 360  $cm^{-1}$  show the out-of-plane bending modes of the ring carbons. The in-plane ring bending vibrations are observed at 798, 796, 792, 769, 768 and 766  $cm^{-1}$ . The other theoretically calculated C–C–C out-of-plane and in-plane bending modes have been found to be consistent with the recorded spectral values. The ring breathing mode is assigned at 1000  $cm^{-1}$  owing to its characteristic intensity and depolarization features in the Raman spectrum. In the case of 2BMX the Raman frequency at 1070, 1069 and 1066  $cm^{-1}$  assigned to ring breathing mode [13]. In the present case a very strong FT-IR band at 1078  $cm^{-1}$  and a weak FT-Raman band at 983  $cm^{-1}$  is assigned to ring breathing mode.

**Fig 3. FT-Raman spectra of 2BMX**

(a) Calculated (b) Observed with B3LYP/6-311+G\*\*

In order to reduce the overall deviation between the unscaled and observed fundamental frequencies, scale factors were applied in the normal coordinate analysis and the

### C-C vibrations

The C–C aromatic stretch, predicted at  $1636\text{ cm}^{-1}$  is in excellent agreement with experimental observation of FT-Raman value at  $1649\text{ cm}^{-1}$ . The theoretically calculated C–C out-of-plane and in-plane bending modes have been found to be consistent with the recorded spectral values.

### C–Br vibrations

The assignments of C–Br stretching and deformation vibrations have been made on the basis of the calculated TED and by comparison with similar molecules and benzene derivatives [14]. In FT-Raman spectrum of 2BMX the medium strong band at  $256\text{ cm}^{-1}$  is assigned to C–Br stretching vibration coupled with ring deformation. The theoretical wavenumber of this band  $257\text{ cm}^{-1}$  coincides well with the experimental, and the calculated TED confirms this assignment [15,16]. The C–Br stretching also contributes to the band observed at 526, 525 and  $524\text{ cm}^{-1}$  in FTIR spectrum. In Infrared spectrum, involve some contribution from the C–Br stretching vibration. The C–Br out-of-plane bending and in-plane bending vibrations are assigned to the Raman bands at 254 and 218,  $213\text{ cm}^{-1}$ , respectively.

### Methyl group vibrations

The title molecule 2BMX, under consideration possesses two  $\text{CH}_3$  groups in first and third position of the ring. For the assignments of  $\text{CH}_3$  group frequencies one can expect that nine fundamentals can be associated to each  $\text{CH}_3$  group, namely the symmetrical stretching in  $\text{CH}_3$  ( $\text{CH}_3$  sym. stretch) and asymmetrical stretching ( $\text{CH}_3$  asym. stretch), in-plane stretching modes (i.e. in-plane hydrogen stretching mode); the symmetrical ( $\text{CH}_3$  sym. deform), and asymmetrical ( $\text{CH}_3$  asym. deform) deformation modes; the in-plane rocking ( $\text{CH}_3$  ipr) out-of-plane rocking ( $\text{CH}_3$  opr) and twisting ( $\text{tCH}_3$ ) bending modes. For the  $\text{CH}_3$  group compounds, the mode appears in the range  $2825\text{--}2870\text{ cm}^{-1}$ , lower in magnitude compared to its value in  $\text{CH}_3$  compounds whereas the two modes for both the types of compounds lie in the same region  $3100\text{--}3000\text{ cm}^{-1}$ . The FT-Raman band at 3112, 3057, 3056 and  $3053\text{ cm}^{-1}$  represents asymmetric and symmetric  $\text{CH}_3$  stretching vibrations of the methyl group in 2BMX [17]. In the case 2BMX, the asymmetric in-plane bending vibration have been identified at 1210, 1206 and  $1204\text{ cm}^{-1}$  and the asymmetric out of-plane bending vibration have been identified at  $1145\text{ cm}^{-1}$  in FT-Raman. The rocking vibration of  $\text{CH}_3$  has been identified at 1026, 1025 and  $1023\text{ cm}^{-1}$ . In the present case the molecule possess two  $\text{CH}_3$  stretching frequencies at 1458, 1456,  $1453\text{ cm}^{-1}$  and 1454, 1453 and  $1450\text{ cm}^{-1}$  in FT-Raman and FTIR spectra, respectively. The theoretically calculated value by B3LYP method using 6-311+G\*\* basis set have been identified the asymmetric and symmetric out-of-plane bending modes of  $\text{CH}_3$  group at 1339 and  $1337\text{ cm}^{-1}$ . The  $\text{CH}_3$  torsional mode could be assigned at  $161\text{ cm}^{-1}$ . It is to be noted here that this is a pure mode.

### Mulliken population analysis

The values of the Mulliken's atomic charges on each atom of the title compound were also obtained with the help of B3LYP level of the theory incorporating 6-311+G\*\* basis set. The total atomic charges on each atom of the title compound are presented in Table 6.

### First-order hyperpolarizability calculations

The first-order hyperpolarizabilities ( $\beta_0$ ) of this novel molecular system, and related properties  $\beta_0$ ,  $\alpha_0$  and  $\Delta\alpha$  of 2BMX were calculated using B3LYP/6-311+G\*\* basis set, based on the finite-field approach. In the presence of an applied electric field, the energy of a system is a function of the electric field. Polarizabilities and hyperpolarizabilities characterize the response of a system in an applied electric field [18]. They

determine not only the strength of molecular interactions (long-range inter induction, dispersion force, etc.) as well as the cross sections of different scattering and collision process but also the nonlinear optical properties (NLO) of the system [19,20]. First-order hyperpolarizability is a third rank tensor that can be described by  $3\times 3\times 3$  matrix. The 27 components of the 3D matrix can be reduced to 10 components due to the Kleinman symmetry [21]. It can be given in the lower tetrahedral format. It is obvious that the lower part of the  $3\times 3\times 3$  matrixes is a tetrahedral. The components of  $\beta$  are defined as the coefficients in the Taylor series expansion of the energy in the external electric field. When the external electric field is weak and homogeneous, this expansion becomes:

$$E = E^0 - \mu_{\alpha} F - 1/2\alpha_{\alpha\beta} F_{\alpha} F_{\beta} - 1/6\beta_{\alpha\beta\gamma} F_{\alpha} F_{\beta} F_{\gamma} + \dots$$

The total static dipole moment is

$$\mu = (\mu_x^2 + \mu_y^2 + \mu_z^2)^{1/2}$$

and the average hyperpolarizability is

$$\beta_0 = (\beta_x^2 + \beta_y^2 + \beta_z^2)^{1/2}$$

and

$$\beta_x = \beta_x + \beta_{xyy} + \beta_{xzz}$$

$$\beta_y = \beta_{yyy} + \beta_{xyy} + \beta_{xzz}$$

$$\beta_z = \beta_x + \beta_{xyy} + \beta_{xzz}$$

The B3LYP/6-311+G\*\* calculated first-order hyperpolarizability of 2BMX is  $1.0574\times 10^{-30}$  esu is shown in Table 7.

Electronic excitation energies, oscillator strength and nature of the respective excited states were calculated by the closed-shell singlet calculation method and are summarized in Table 8. Fig 4 shows the highest occupied molecule orbital (HOMO) and lowest unoccupied molecule orbital (LUMO) of 2BMX. Orbital involved in the electronic transition for (a) HOMO–0 (b) LUMO+0 (c) HOMO–1 (d) LUMO+1 (e) LUMO+2 is represented in Fig 5. The NLO responses can be understood by examining the energetic of frontier molecular orbitals. There is an inverse relationship between hyperpolarizability and HOMO–LUMO.

HOMO energy =  $-0.001\text{ a.u}$

LUMO energy =  $0.014\text{ a.u}$

HOMO–LUMO energy gap =  $0.015\text{ a.u}$

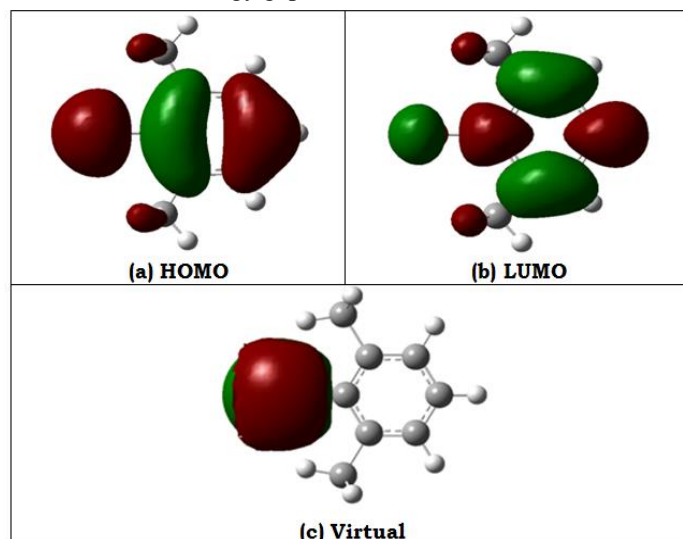
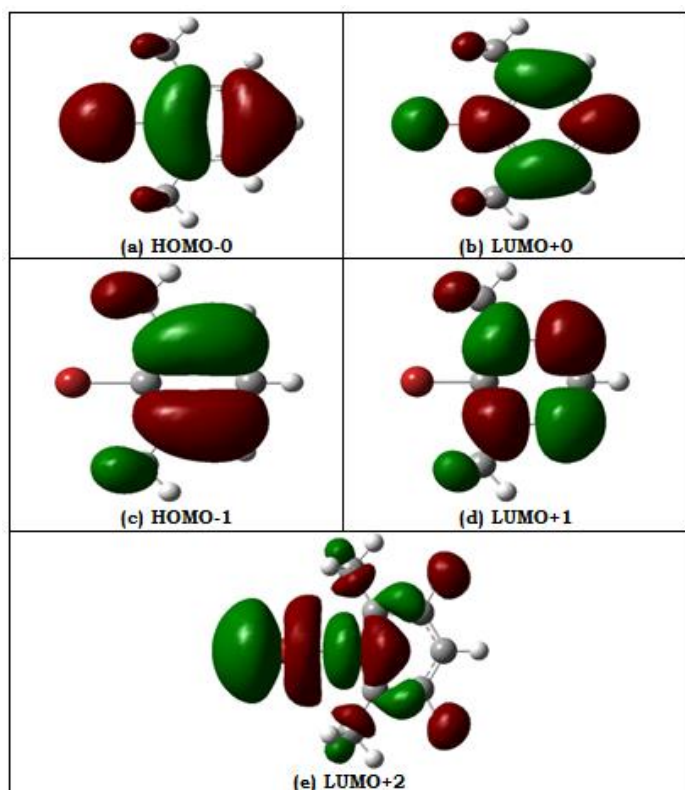


Fig 4. Representation of the orbital involved in the electronic transition for (a) HOMO (b) LUMO (c) Virtual



**Fig 5. Representation of the orbital involved in the electronic transition for (a) HOMO-0 (b) LUMO+0 (c) HOMO-1 (d) LUMO+1 (e) LUMO+2**

### Conclusions

Attempts have been made in the present work for the proper frequency assignments for the compound 2BMX. The FT-IR and FT-Raman spectra were recorded. The equilibrium geometries and harmonic frequencies of 2BMX were determined and analysed at DFT level of theories utilizing B3LYP/6-311+G\*\* basis sets. The difference between the observed and scaled wave number values of most of the fundamentals is very small. Any discrepancy noted between the observed and the calculated frequencies may be due to the fact that the calculations have been actually done on single molecules in the gaseous state contrary to the experimental values recorded in the presence of intermolecular interactions. The values of the Mulliken's atomic charges on each atom of the title compound were also obtained. The first-order hyperpolarizability ( $\beta_{total}$ ) of 2BMX was calculated and found to be  $1.0574 \times 10^{-30}$  esu. Electronic excitation energies, oscillator strength and nature of the respective excited states were calculated by the closed-shell singlet calculation method.

### References

1. M. Castella-Ventura, E. Kassab, G. Buntinx, O. Poizat, Phys. Chem. Chem. Phys., 2(2000) 4682.
2. D.N. Shin, J.W. Hahn, K.H. Jung, T.K. Ha, J.Raman Spectrosc., 29 (1998) 245.

3. B. Giese, D. McNaughton, Phys. Chem. Chem. Phys., 4 (2002) 5161.
4. M. J. Frisch, G. W. Trucks, H. B. Schlegel, G. E. Scuseria, M. A. Robb, J. R. Cheeseman, G. Scalmani, V. Barone, B. Mennucci, G. A. Petersson, H. Nakatsuji, M. Caricato, X. Li, H. P. Hratchian, A. F. Izmaylov, J. Bloino, G. Zheng, J. L. Sonnenberg, M. Hada, M. Ehara, K. Toyota, R. Fukuda, J. Hasegawa, M. Ishida, T. Nakajima, Y. Honda, O. Kitao, H. Nakai, T. Vreven, J. A. Montgomery, Jr., J. E. Peralta, F. Ogliaro, M. Bearpark, J. J. Heyd, E. Brothers, K. N. Kudin, V. N. Staroverov, R. Kobayashi, J. Normand, K. Raghavachari, A. Rendell, J. C. Burant, S. S. Iyengar, J. Tomasi, M. Cossi, N. Rega, J. M. Millam, M. Klene, J. E. Knox, J. B. Cross, V. Bakken, C. Adamo, J. Jaramillo, R. Gomperts, R. E. Stratmann, O. Yazyev, A. J. Austin, R. Cammi, C. Pomelli, J. W. Ochterski, R. L. Martin, K. Morokuma, V. G. Zakrzewski, G. A. Voth, P. Salvador, J. J. Dannenberg, S. Dapprich, A. D. Daniels, O. Farkas, J. B. Foresman, J. V. Ortiz, J. Cioslowski, and D. J. Fox, Gaussian, Inc., Wallingford CT, 2009.
5. A.D. Becke, J. Chem. Phys., 98 (1993) 5648.
6. C. Lee, W. Yang, R.G. Parr, Phys. Rev., B37 (1988) 785.
7. P. Pulay, G. Fogarasi, G. Pongor, J.E. Boggs, A. Vargha, J.Am. Chem. Soc., 105 (1983) 7037.
8. B. Wojtkowiak, M. Chabanel, Spectrochimie Moleculaire Technique et Documentation, Paris, 1977.
9. G. Keresztury, S. Holly, J. Varga, G. Besenyi, A.Y. Wang, J.R. Durig, Spectrochim. Acta 49A (1993) 2007.
10. G. Keresztury, in: J.M. Chalmers, P.R. Griffiths (Eds.), Raman Spectroscopy: Theory in Handbook of Vibrational Spectroscopy, vol.1, John Wiley & Sons Ltd., 2002.
11. P. Pulay, G. Fogarasi, G. Pongor, J.E. Boggs, A. Vargha, J.Am. Chem. Soc., 105 (1983) 7037.
12. R. Zwarich, J. Smolarck, L. Goodman, J. Mol. Spectrosc. 38 (1971) 336.
13. D.N. Singh, I.D. Singh, R.A. Yadav, Ind. J. Phys. B 76 (3) (2002) 307.
14. W. Zierkiewicz, D. Michalska, Th. Zeegers-Huyskens, J. Phys. Chem. A 104 (2000) 11685.
15. Mehmet Karabacak and Mehmet Cinar, Spectrochimica Acta Part A: Molecular and Biomolecular Spectroscopy, 86 (2012) 590-599.
16. E.F. Mooney, Spectrochim. Acta 20 (1964) 1021.
17. G. Varsanyi, Vibrational Spectra of 700 Benzene Derivatives, vol. I-II, Akademiai Kiado, Budapest, 1973.
18. C.R. Zhang, H.S. Chen, G.H. Wang, Chem. Res. Chin. U. 20 (2004) 640-646.
19. Y. Sun, X. Chen, L. Sun, X. Guo, W. Lu, J. Chem. Phys. Lett. 381 (2003) 397-403.
20. O. Christiansen, J. Gauss, J.F. Stanton, J. Chem. Phys. Lett. 305 (1999) 147-155.
21. D.A. Kleinman, Phys. Rev. 1962;126,1977.